

Meta-analytic activation maps can help identify affective processes captured by contrast-based task fMRI: the case of threat-related facial expressions

M. Justin Kim,^{1,2} Annchen R. Knodt,³ and Ahmad R. Hariri³

¹Department of Psychology, Sungkyunkwan University, Seoul 03063, South Korea

²Center for Neuroscience Imaging Research, Institute for Basic Science, Suwon 16419, South Korea, and

³Laboratory of NeuroGenetics, Department of Psychology and Neuroscience, Duke University, Durham, NC 27708 USA

Correspondence should be addressed to M. Justin Kim, Department of Psychology, Sungkyunkwan University, Seoul 03063, South Korea.

E-mail: minuekim@skku.edu.

Abstract

Meta-analysis of functional magnetic resonance imaging (fMRI) data is an effective method for capturing the distributed patterns of brain activity supporting discrete cognitive and affective processes. One opportunity presented by the resulting meta-analysis maps (MAMs) is as a reference for better understanding the nature of individual contrast maps (ICMs) derived from specific task fMRI data. Here, we compared MAMs from 148 neuroimaging studies representing emotion categories of fear, anger, disgust, happiness and sadness with ICMs from fearful > neutral and angry > neutral faces from an independent dataset of task fMRI ($n = 1263$). Analyses revealed that both fear and anger ICMs exhibited the greatest pattern similarity to fear MAMs. As the number of voxels included for the computation of pattern similarity became more selective, the specificity of MAM–ICM correspondence decreased. Notably, amygdala activity long considered critical for processing threat-related facial expressions was neither sufficient nor necessary for detecting MAM–ICM pattern similarity effects. Our analyses suggest that both fearful and angry facial expressions are best captured by distributed patterns of brain activity, a putative neural correlate of threat. More generally, our analyses demonstrate how MAMs can be leveraged to better understand affective processes captured by ICMs in task fMRI data.

Key words: fMRI; meta-analysis map; emotion; fear; anger; facial expression

Introduction

Understanding how emotions map onto human brain function is a long-standing aim of affective neuroscience. To achieve this goal, affective neuroscientists have heavily employed functional magnetic resonance imaging (fMRI) to examine whether different properties of emotion based on existing theories—such as a valence/arousal dimension (Russell, 1980) or basic emotion categories (Ekman, 1992)—may be reflected in patterns of brain activity. Early fMRI studies that aimed to elucidate the neural representations of categorical emotions focused on the amygdala because of its demonstrated importance in aversive learning as exemplified through the acquisition of a conditioned fear response (LeDoux, 1993; Maren, 2001). However, fMRI studies have yielded mixed results wherein amygdala activity may be elicited by not only threat-related emotions (e.g. fear and anger) but also other categories of emotion (e.g. happiness and sadness) (Davis and Whalen, 2001).

In fact, it has been suggested that amygdala activity alone does not provide a sufficient level of specificity in distinguishing

emotion categories (Fitzgerald *et al.*, 2006). More generally, fMRI studies examining discrete emotion categories have not revealed correspondingly discrete brain regions (Lindquist *et al.*, 2012). In contrast, recent research employing multivoxel pattern analysis (MVPA) offers evidence that discrete emotion categories may be best represented by distributed patterns of activity across the brain (Kassam *et al.*, 2013; Kragel and LaBar, 2015; Kragel *et al.*, 2019; Peelen *et al.*, 2010; Saarimäki *et al.*, 2016; but see Barrett and Satpute, 2019).

A rapidly expanding portfolio of fMRI studies has allowed for a series of computational methods designed to generate voxel-wise meta-analysis maps (MAMs) of brain activity associated with specific cognitive and affective processes (Eickhoff *et al.*, 2009; Kober and Wager, 2010; Yarkoni *et al.*, 2011). MAMs typically share the same coordinate or stereotaxic space [e.g. Montreal Neurological Institute (MNI) or Talairach] as individual contrast maps (ICMs), which represent subject-level brain activity associated with a study-specific contrast of interest. As such, MAMs could

Received: 28 October 2019; Revised: 30 October 2021; Accepted: 7 February 2022

© The Author(s) 2022. Published by Oxford University Press.

This is an Open Access article distributed under the terms of the Creative Commons Attribution-NonCommercial License

(<https://creativecommons.org/licenses/by-nc/4.0/>), which permits non-commercial re-use, distribution, and reproduction in any medium, provided the original work is properly cited. For commercial re-use, please contact journals.permissions@oup.com

provide a reference map for a given mental process or behavior. For example, ICMs of a typical emotion category, such as fear, should show patterns of brain activity more similar to MAMs of the corresponding category (i.e. fear) than other categories (e.g. disgust or sadness). In other words, if affective information for fear is indeed represented in brain activity for fear ICMs, they should correspond to the associated MAMs for fear. This not only presents a testable prediction but also an opportunity to refine ICMs (through pattern similarity analysis with MAMs) in a fashion that maximizes their ability to capture brain activity supporting a specific mental process.

In this study, we aimed to test a simple idea: would an ICM of a given emotion category show greater similarity to the MAM of the same category over others? There are at least three conditions that serve as a prerequisite for such an examination: (i) MAMs from voxel-wise meta-analyses of fMRI data, (ii) category-specific ICMs from a study with a sufficiently large sample size and (iii) independence between the MAMs and ICMs—that is, the ICMs selected for testing should not have been used in the generation of the MAMs. Here, we take advantage of datasets that satisfy these conditions. First, Wager *et al.* (2015) have conducted a computational meta-analysis of 148 functional neuroimaging studies to generate MAMs for five emotion categories: fear, anger, disgust, happiness and sadness. Second, the Duke Neurogenetics Study (DNS) offers a large independent dataset ($n = 1263$) of ICMs for fear, anger, surprise and neutral emotions from a widely utilized face-matching task. Importantly, none of the ICMs from the DNS were included in the generation of MAMs.

Also of importance is considering neural representations of emotion in the context of experience *vs* perception. Measuring brain activity when a person is experiencing (i.e. feeling) anger may not necessarily be the same as when they are perceiving (i.e. looking at) angry facial expressions of others. Affective neuroscience suggests the experience and perception of emotions yield both shared and distinct neural correlates (see Kober *et al.*, 2008; Lindquist *et al.*, 2012 for meta-analysis and review). It is worth noting then that the ICMs we use in the present analyses represent correlates of the perception of emotional facial expressions, whereas the MAMs were computed from fMRI data derived from both the experience and perception of emotions (see Supplementary Figure S1 of Wager *et al.* 2015 for details). Taking these differences into account may be key to understanding the present MAM-ICM associations.

Based on the existing literature, we hypothesized that ICMs for fear and anger would show the greatest pattern similarity to MAMs for fear and anger, respectively. Moreover, we sought to examine the possibility that affective information pertaining to emotion categories is distributed across the whole brain by systematically varying the number of voxels submitted for pattern similarity analysis. Finally, given the prominence of the amygdala in the affective neuroscience literature (Adolphs *et al.*, 1995; Phelps and LeDoux, 2005; Costafreda *et al.*, 2008; Kim *et al.*, 2011), we tested whether amygdala activity specifically was either sufficient or necessary to produce the MAM-ICM pattern similarity observed in whole-brain analyses.

Methods

Participants

One thousand two-hundred and sixty-three participants (717 women, 19.7 ± 1.3 years of age) successfully completed the DNS between January 2010 and November 2016, including an fMRI

task eliciting threat-related brain activity. All participants provided written informed consent according to the Duke University Medical Center Institutional Review Board. To be eligible for the DNS, participants were required to be free of the following conditions: (i) medical diagnoses of cancer, stroke, head injury with loss of consciousness, untreated migraine headaches, diabetes requiring insulin treatment, or chronic kidney or liver disease; (ii) use of psychotropic, glucocorticoid or hypolipidemic medication and (iii) conditions affecting cerebral blood flow and metabolism (e.g. hypertension). As DNS followed a standardized procedure, we note that the following description of the methods is also described elsewhere (e.g. Kim *et al.*, 2018).

Face-matching task

The face-matching task used in the DNS consisted of four task blocks interleaved with five control blocks. A total of four emotion categories were used for each task block: fear (F), anger (A), surprise (S) and neutral (N), taken from a standardized facial expression set (Ekman and Friesen, 1976). Participants viewed the task blocks in one of four randomly assigned orders as determined by a Latin Square (i.e. FNAS, NFSA, ASFN and SANF). During task blocks, participants viewed a trio of faces that belonged to the same emotional category (e.g. all three faces displayed fearful expressions in fear blocks) and matched one of two faces identical to a target face. Each trial in the task blocks lasted for 4 s with a variable interstimulus interval of 2–6 s (mean = 4 s), for a total block length of 48 s. The control blocks consisted of six geometric shape trios, which were presented for 4 s with a fixed interstimulus interval of 2 s for a total block length of 36 s. Each block was preceded by a brief instruction ('Match faces' or 'Match shapes') lasting 2 s. Total task time was 390 s.

fMRI data acquisition

Each participant was scanned using one of the two identical research-dedicated GE MR750 3T scanner equipped with high-power high-duty-cycle 50-mT/m gradients at 200 T/m/s slew rate and an eight-channel head coil for parallel imaging at high bandwidth up to 1 MHz at the Duke-UNC Brain Imaging and Analysis Center. A semi-automated high-order shimming program was used to ensure global field homogeneity. A series of 34 interleaved axial functional slices aligned with the anterior commissure-posterior commissure plane were acquired for full-brain coverage using an inverse-spiral pulse sequence to reduce susceptibility artifacts (repetition time (TR), echo time (TE)/flip angle = 2000 ms/30 ms/60°; field of view (FOV) = 240 mm; $3.75 \times 3.75 \times 4$ mm voxels; interslice skip = 0). Four initial radiofrequency excitations were performed (and discarded) to achieve steady-state equilibrium. To allow for spatial registration of each participant's data to a standard coordinate system, high-resolution three-dimensional T1-weighted structural images were obtained in 162 axial slices using a 3D Ax FSPGR BRAVO sequence (TR/TE/flip angle = 8.148 ms/3.22 ms/12°; voxel size = $0.9375 \times 0.9375 \times 1$ mm; FOV = 240 mm; interslice skip = 0; total scan time = 4 min and 13 s). In addition, high-resolution structural images were acquired in 34 axial slices coplanar with the functional scans and used for spatial registration for participants without Ax FSPGR BRAVO images (TR/TE/flip angle = 7.7 s/3.0 ms/12°; voxel size = $0.9 \times 0.9 \times 4$ mm; FOV = 240 mm, interslice skip = 0).

fMRI data preprocessing

Anatomical images for each subject were skull-stripped, intensity-normalized and non-linearly warped to a study-specific

average template in the standard stereotactic space of the MNI template using Advanced Normalization Tools (ANTs) (Klein et al., 2009). BOLD time series for each subject were processed in AFNI (Cox, 1996). Images for each subject were despiked, slice time-corrected, realigned to the first volume in the time series to correct for head motion, coregistered to the anatomical image using FSL's Boundary Based Registration (Greve and Fischl, 2009), spatially normalized into MNI space using the non-linear warp from the anatomical image, resampled to 2 mm isotropic voxels, and smoothed to minimize noise and residual difference in gyral anatomy with a Gaussian filter, set at 6 mm full-width at half-maximum. All transformations were concatenated so that a single interpolation was performed. Voxel-wise signal intensities were scaled to yield a time series mean of 100 for each voxel. Volumes exceeding 0.5 mm framewise displacement (FD) or 2.5 standardized temporal derivative of root mean square (RMS) variance over voxels (DVARs) (Power et al., 2014; Nichols, 2017) were censored.

Individual contrast maps

The AFNI program *3dREMLfit* (<http://afni.nimh.nih.gov/>) was used to fit a general linear model for first-level fMRI data analyses. To obtain emotion-specific parameter estimates, we explicitly modeled each respective task block (convolved with the canonical hemodynamic response function) along with the adjacent half of the preceding and following control blocks and a first-order polynomial regressor to account for low-frequency noise. This allowed for the estimation of the individual task block parameters while minimizing the influence of adjacent task blocks as well as low-frequency noise across the entire run. The resulting parameter estimates for the fear and anger task blocks and the neutral task blocks were then subtracted to obtain the fearful > neutral and angry > neutral faces ICMs (henceforth referred to as ICM-F and ICM-A, respectively), and these ICMs were used to compute pattern similarity with the MAMs. The contrast surprise > neutral was omitted from the present study, because a corresponding surprise MAM does not exist. ICMs were then used in second-level random-effects models in SPM12 (<http://www.fil.ion.ucl.ac.uk/spm>) accounting for scan-to-scan and participant-to-participant variability to determine mean emotion-specific activity using one-sample t-tests. A statistical threshold of $P < 0.05$, family-wise error (FWE)-corrected across the whole brain was applied to the fearful > neutral and angry > neutral contrasts, respectively. The ICMs are available by reasonable request, following the data-sharing procedures through our website (<https://www.haririlab.com/projects/procedures.html>).

fMRI quality assurance criteria

Quality control criteria for inclusion of a participant's imaging data were as follows: >5 volumes for each condition of interest retained after censoring for FD and DVARs and sufficient temporal signal-to-noise ratio (SNR) within the bilateral amygdala, defined as no greater than 3 s.d. below the mean of this value across participants. The amygdala was defined using a high-resolution template generated from the 168 Human Connectome Project datasets (Tyszka and Pauli, 2016). Additionally, data were only included in further analyses if the participant demonstrated sufficient engagement with the task, defined as achieving at least 75% accuracy during the task blocks.

Meta-analysis maps

The MAMs utilized in the present study are based on a meta-analysis of 148 fMRI studies of emotional categories (Wager et al., 2015). The MAMs were generously made available by these study authors on their website (<https://canlabweb.colorado.edu/fmri-resources.html>). In brief, the original meta-analysis consisted of five distinct emotion categories (fear, anger, disgust, sadness and happiness), and MAMs for each category were generated in standard MNI space using a hierarchical Bayesian model that summarizes the expected frequency of activation for a given emotion category. The values that each voxel of the MAMs assumes are reflective of this information, such that taking the integral over any area of the brain represents the expected number of activation centers for all studies of a given emotion category (Wager et al., 2015). The overall findings indicated that brain activity patterns that are diagnostic of distinct categories of emotion are characterized as widespread (i.e. distributed across not only multiple brain regions but also many neural systems that span cognitive, perceptual and motor functions). For the purposes of the present study, higher-intensity voxel values of the MAMs indicate a greater likelihood with which the MAMs correspond to a given emotion category. Detailed characteristics of the MAMs are described in the original study (Wager et al., 2015). In brief, the 148 studies included 377 unique study activation maps; out of those, 97 and 69 maps were used to generate MAMs for fear and anger, respectively. The study activation maps were contrasting an emotion-related condition to a less intense or affectively neutral comparison condition. The majority of the individual studies presented the experimental stimuli visually. For fear and anger MAMs, over half of the studies used faces/ facial expressions in some capacity, followed by pictures, film and words (see Supplementary Figure S1 of Wager et al. 2015 for details). Importantly, none of the 148 studies that were included in this meta-analysis overlapped with the DNS, ensuring independence across MAMs and ICMs (the MAMs included studies published from 1993 to 2011; the first study using the ICMs from the emotional face-matching task in the DNS was published in 2012).

MAM-ICM pattern similarity computation

For quantifying MAM-ICM pattern similarity, we adopted a modified version of an approach described by Shahane et al. (2019). First, prior to each analysis, ICMs were masked with the target MAMs, to match the number of non-zero voxels. Then, for each MAM-ICM pair, all non-zero voxels were vectorized and demeaned in order to compute their correlation coefficients, which were subsequently converted to z scores using Fisher's r -to- z transformation (Figure 1). Computation of correlation coefficients across vectorized voxels was achieved with *3dcorr* implemented within AFNI (Cox, 1996). Higher z scores indicated greater pattern similarity between a given MAM-ICM pair. Since there were five MAMs, a total of 5 z scores were computed for each of two ICMs for each participant. As we were primarily interested in how well a given ICM (e.g. ICM-F) aligned with its corresponding MAM (e.g. MAM-F) above and beyond other MAMs, the z scores were compared across the MAMs. Two models were generated to test this: (i) a one-way repeated-measures analysis of variance (ANOVA) where z scores for a given ICM and MAMs for each of the five emotion categories were compared and (ii) a paired t-test where z scores for a given ICM and MAMs for fear and anger, specifically, were compared. The latter model was used to specifically focus on the two emotion categories that were available as both ICMs and MAMs. Analyses were done separately for ICM-F

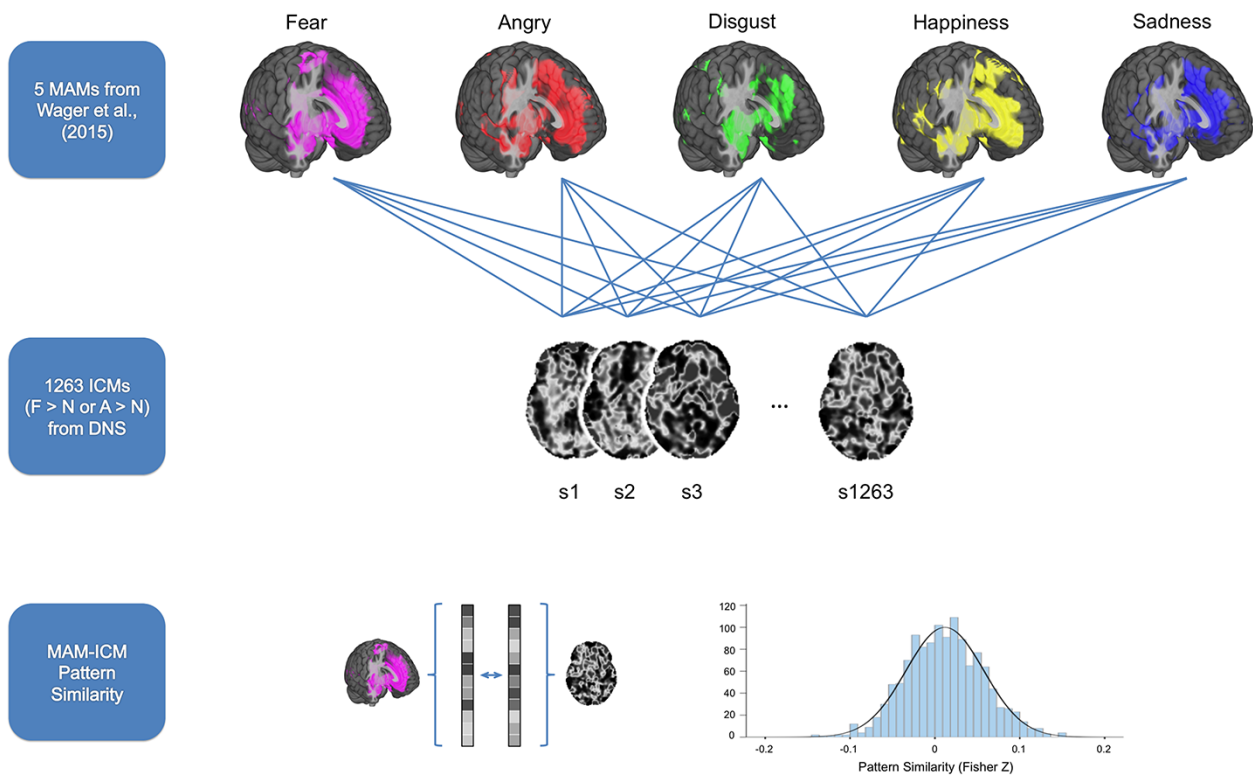


Fig. 1. Summary of data analysis procedures used for assessing MAM–ICM pattern similarity. ICMs for fearful > neutral and angry > neutral derived from 1263 participants performing an emotional face-matching task were compared with five MAMs corresponding to different categories of emotion from Wager et al. (2015). For each MAM–ICM pair, all non-zero voxels were vectorized in order to compute their correlation coefficient, which was subsequently converted to z scores using Fisher’s r -to- z transformation.

and ICM-A. In this way, we could confirm the a priori prediction that ICM-F would correspond better to the MAM-F, above and beyond the MAMs of other emotion categories; then, the same procedure was applied to test whether ICM-A would show increased pattern similarity to the MAM-A compared to other MAMs.

To test whether the number of voxels included in the analyses impacted the results, MAM–ICM pattern similarity measures were computed repeatedly using MAMs at different thresholds. The threshold was systematically varied, ranging from unthresholded to 0.1 intensity values, which represents the expected frequency of activation centers for an emotion category, with each step increasing the threshold by 2-fold (i.e. unthresholded–0.001–0.005–0.01–0.05–0.1). It is notable that there was a general tendency for cortical areas to become reduced as a function of increased MAM threshold, while the amygdala was among the last regions to remain, regardless of emotion category (Figure 2). Effect sizes from the analyses that compared a given ICM across different MAMs (partial η^2 for ANOVA, Cohen’s d for t -test) were used to describe the effect of applying different thresholds on the pattern similarity metrics.

Finally, to test the contribution of amygdala activity specifically on the pattern similarity results from the main analyses, two sets of subsequent analyses were performed on the data. First, each MAM–ICM pair was masked with an anatomical region of interest (ROI) of the amygdala, divided into basolateral and centromedial subregions (Tyszka and Pauli, 2016), which then underwent the same procedure described above using only the amygdala voxels (here, only unthresholded MAM voxels were used). In a separate set of analyses, each MAM–ICM

pair was masked with a reversed mask of the anatomical ROI, such that all amygdala voxels were removed from further analysis. Then, the same procedure as the main analyses was repeated for the amygdala-excluded MAM–ICM pairs. The latter analysis tested the prediction that if the amygdala voxels contain important information about distinct emotion categories, then it would yield decreased pattern similarity metrics for corresponding MAM–ICM pairs. To supplement the MAM–ICM findings, the aforementioned analyses were repeated by replacing ICMs with group contrast maps (fearful > neutral and angry > neutral) derived from second-level random-effects models (see supplementary data).

Results

ICMs: fearful > neutral and angry > neutral

Across the entire brain, both ICMs yielded significant activity in the amygdala, supramarginal gyrus/angular gyrus extending to the superior temporal sulcus (STS), and inferior frontal gyrus (IFG). The fearful > neutral ICMs also revealed significantly increased activity in the occipital pole and the inferior temporal gyrus (ITG). Significantly activated amygdala voxel clusters were isolated within the amygdala proper and not a part of a larger cluster that extends to other brain regions (Figure 3, Table 1).

Whole-brain MAM–ICM pattern similarity for fear

Overall, there was significant pattern similarity between ICM-F and MAM-F ($M = 0.0065$, $s.d. = 0.03$, $[\min, \max] = [-0.11, 0.11]$; one-sample t -test: $t_{(1262)} = 7.57$, $P < 0.000001$, $d = 0.21$). This effect remained significant when the MAMs were thresholded at varying

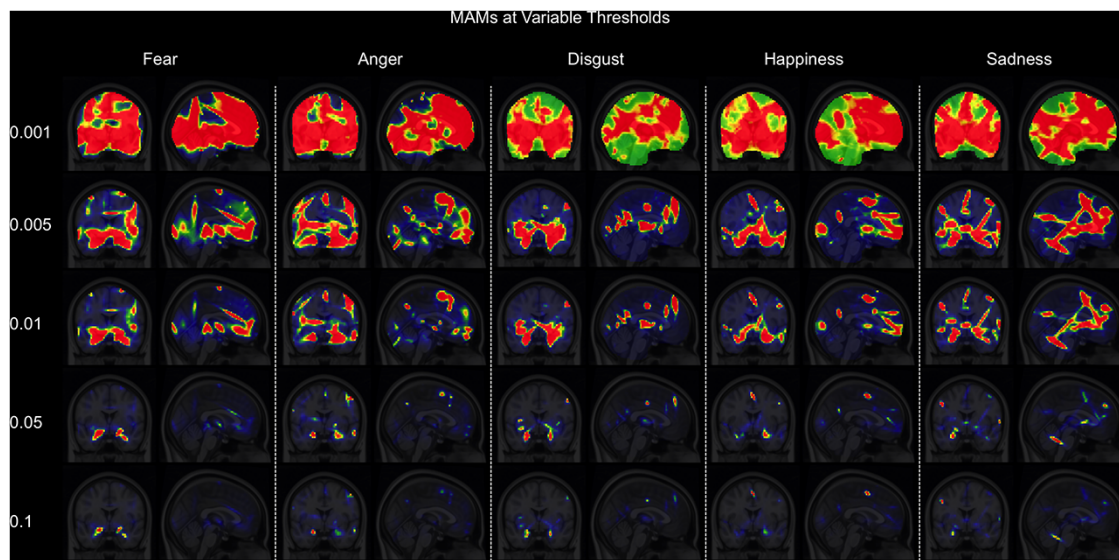


Fig. 2. Five emotion-specific MAMs at systematically varied thresholds. Voxels that survived increasingly stringent thresholds (i.e. the higher intensity values noted on the left-hand side) are depicted by hotter colors. Intensity values indicate the expected frequency of activation centers for an emotion category (see Wager et al., 2015 for details).

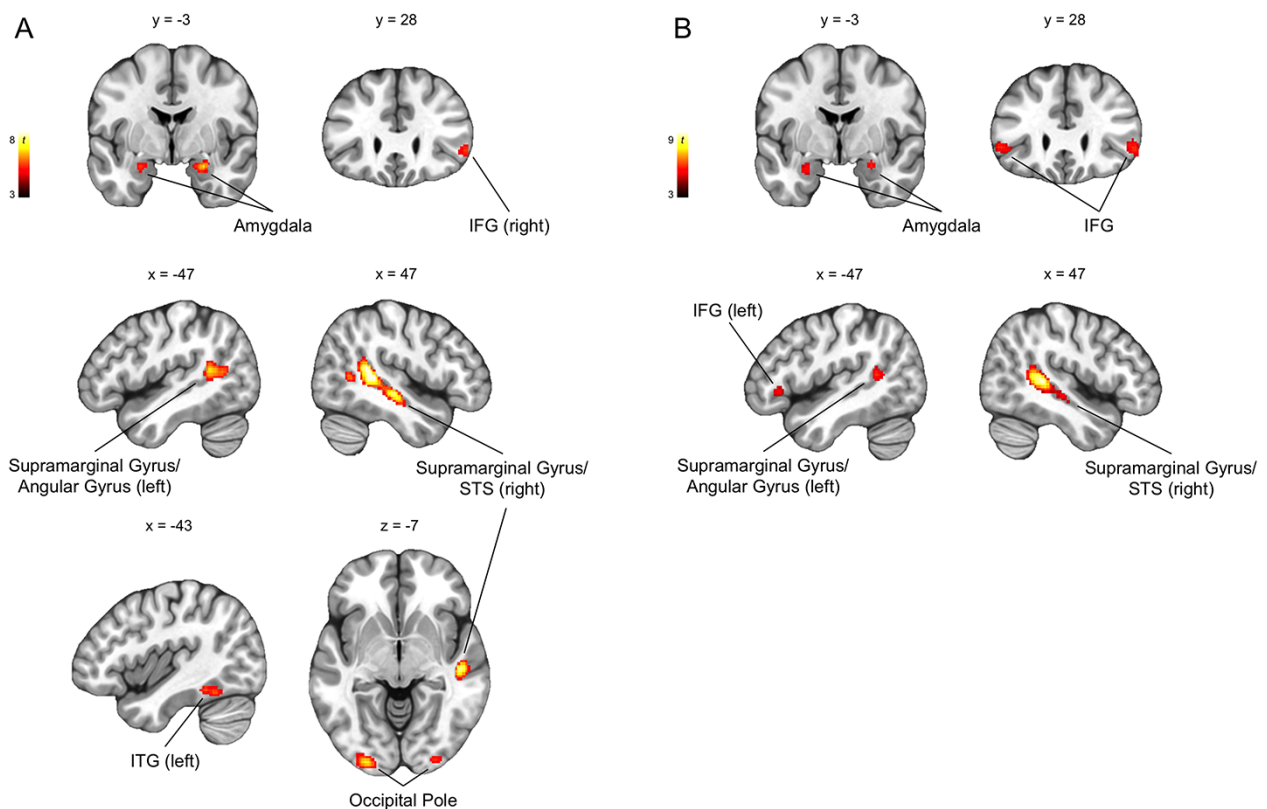


Fig. 3. Group-level whole-brain responses from 1263 participants performing an emotional face-matching task ($P < 0.05$, FWE-corrected for the whole brain; $k \geq 30$ are visualized). (A) Brain regions that showed significantly increased activity to fearful > neutral included the amygdala, supramarginal gyrus/angular gyrus/STS, IFG, inferior temporal gyrus (ITG) and the occipital pole. (B) Similar brain regions showed significantly increased activity to angry > neutral.

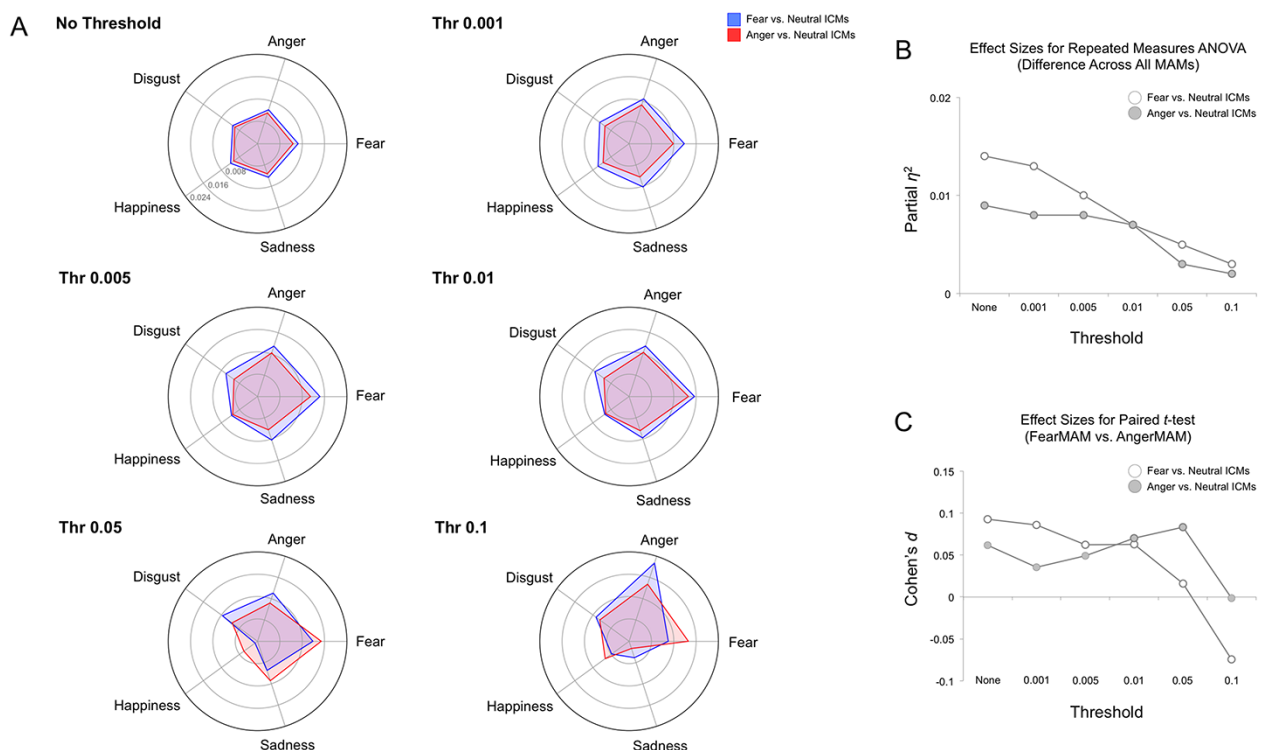
levels (all P s < 0.002), except for one instance (ICM-F and MAM-F pair thresholded at 0.1; $P = 0.16$).

Repeated-measures ANOVA showed significant differences of MAM-ICM pattern similarity for ICM-F across the five MAMs ($F_{(45,048)} = 17.27$, $P < 0.000001$; $\eta_p^2 = 0.014$). Post hoc analysis revealed that pattern similarity for MAM-F was significantly

greater than the other four MAMs (all P s < 0.002). This finding remained when the threshold was increased to 0.01 (i.e. less voxels were selected); however, this effect was no longer observable when the threshold was further increased. Paired t -tests showed similar findings as the ANOVA, such that pattern similarity between ICM-F and MAM-F was significantly greater than

Table 1. Brain regions showing significant activation for the contrasts of fearful > neutral and angry > neutral ($P < 0.05$, FWE-corrected for the whole brain)

Brain region	Side	t	x	y	z	No. of voxels
Fearful > neutral						
Supramarginal gyrus/STS	R	8.1	47	-41	11	1034
Supramarginal gyrus/angular gyrus	L	7.6	-57	-53	-7	537
Occipital pole	L	6.9	-27	-95	7	186
Occipital pole	R	6.1	31	-93	-3	119
Amygdala	R	6.6	25	-3	-19	106
Amygdala	L	5.4	-25	-3	-19	32
ITG	L	6	-43	-51	-17	66
IFG	R	5.5	55	27	-1	49
Angry > neutral						
Supramarginal gyrus/STS	R	8.8	49	-37	5	710
Supramarginal gyrus/angular gyrus	L	6.2	-55	-49	13	173
IFG	R	5.9	53	27	-1	87
IFG	L	6.3	-51	29	-1	79
Amygdala	R	6.6	25	-5	-17	65
Amygdala	L	5.6	-27	-3	-21	30

**Fig. 4.** Whole-brain MAM-ICM pattern similarity for fear and anger. (A) Pattern similarity measures of ICM-F (blue) and ICM-A (red) to each of the five MAMs, summarized by varying threshold levels. Overall, both fear ICMs showed greater pattern similarity with the fear MAM, but this effect disappeared when the threshold was sufficiently high (e.g. 0.1). (B) Plotting the effect sizes from repeated-measures ANOVA showed a gradually declining trend as a function of increased threshold levels. (C) A similar trend was found when the effect sizes from paired t-tests were plotted.

MAM-A ($t_{(1262)} = 3.3$, $P = 0.001$; $d = 0.09$). Again, this effect was observable until the threshold was increased to 0.01. When the threshold was set to the highest level (0.1), an unexpected opposite effect was found such that pattern similarity between ICM-F and MAM-F was significantly less than for ICM-F and MAM-A ($t_{(1262)} = -2.65$, $P = 0.008$; $d = 0.1$).

Effect sizes of the ANOVA and t-test results gradually decreased as a function of increased threshold levels. As ICM-F showed the highest level of pattern similarity to MAM-F over other MAMs, diminishing effect sizes suggest a relative decrease in the

specificity of ICM-F to MAM-F. These findings are summarized in Figure 4 (white bars and circles).

Whole-brain MAM-ICM pattern similarity for anger

Again, there was significant pattern similarity between ICM-A and MAM-A ($M = 0.0036$, $s.d. = 0.02$, $[min, max] = [-0.06, 0.06]$; one-sample t-test: $t_{(1262)} = 6.71$, $P < 0.000001$, $d = 0.19$). This effect persisted regardless of differences in the thresholds applied to the MAMs.

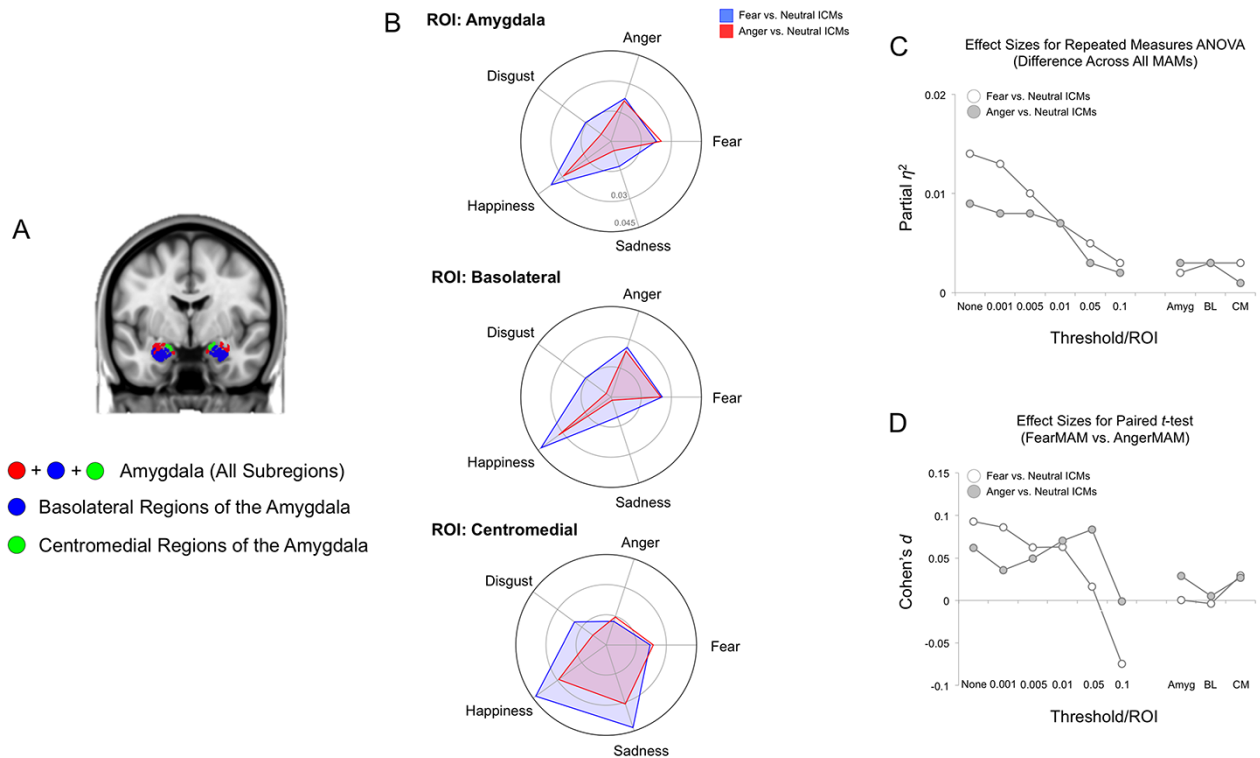


Fig. 5. MAM-ICM pattern similarity for amygdala activity. (A) Anatomical definitions of the amygdala, basolateral amygdala and centromedial amygdala used to select the voxels for ICM analysis (Tyszka and Pauli, 2016). (B) Pattern similarity measures for ICM-F (blue) and ICM-A (red) and each of the five MAMs, summarized by the ROIs used to define the amygdala and its subregions. Overall, neither ICM-F nor ICM-A exhibited pattern similarity with either MAM-F or MAM-A. (C) Plotting the effect sizes from repeated-measures ANOVA showed a very small overall effect, regardless of activation locus (i.e. whole amygdala or subregion). The line graphs on the left represent the findings from the whole-brain pattern similarity analysis (i.e. same as Figure 4B). (D) Similar findings were observed with the very small effect size for the paired t-tests.

Repeated-measures ANOVA showed significant differences of MAM-ICM pattern similarity for ICM-A across the five MAMs ($F_{(45, 048)} = 11.46$, $P < 0.000001$; $\eta_p^2 = 0.009$). Post hoc analysis revealed, however, that ICM-A showed greatest pattern similarity to MAM-F compared to the other four MAMs, including anger (all P s < 0.03). This finding remained when the threshold was increased to 0.05 (i.e. less voxels were selected); however, this effect was no longer observable when the threshold was increased to 0.1. Paired t-tests showed similar findings as the ANOVA, such that pattern similarity between ICM-A and MAM-A was significantly less than for ICM-A and MAM-F ($t_{(1262)} = -2.2$, $P = 0.028$, $d = 0.06$). Again, this effect was observable up until the threshold was increased to 0.05. When the threshold was set to the highest level (0.1), this effect was no longer present.

Effect sizes of the ANOVA results gradually decreased as a function of increased threshold levels. Effect sizes of the t-tests showed a less clear but consistent pattern where the highest threshold (0.1) yielded the smallest effect size. However, as ICM-A showed the highest pattern similarity to MAM-F and not MAM-A, diminishing effect sizes indicate a relative decrease in the specificity of ICM-A to MAM-F. These findings are summarized in Figure 4 (gray bars and circles).

Amygdala MAM-ICM pattern similarity for fear and anger

Repeated-measures ANOVA showed significant differences in pattern similarity in amygdala activity between ICM-F and all five MAMs ($F_{(45, 048)} = 2.86$, $P = 0.022$; $\eta_p^2 = 0.002$). However, post

hoc analysis showed that this effect was driven by an unexpected pattern similarity between ICM-F and the MAM for happiness. This finding remained the same when the analysis was restricted to basolateral or centromedial subregions of the amygdala. Paired t-tests showed similar findings as the ANOVA, such that the pattern similarity between ICM-F and MAM-F was no different from those for MAM-A. Again, this effect remained the same for basolateral or centromedial subregions of the amygdala.

Similarly, amygdala activity from ICM-A significantly differed from all five MAMs ($F_{(45, 048)} = 4.07$, $P = 0.003$; $\eta_p^2 = 0.003$), but the happiness MAM showed the greatest degree of pattern similarity to ICM-A. This effect remained when only the basolateral or centromedial amygdala voxels were considered in the analysis. Once again, pairwise comparison between MAM-F and MAM-A yielded no significant differences in overall or subregional amygdala activity.

The very small effect sizes of the ANOVA and t-test results of the amygdala analyses showed that they were comparable to the whole-brain analyses using the highest threshold levels and not useful in parsing the distinct emotion categories. These findings are summarized in Figure 5.

Non-amygdala MAM-ICM pattern similarity for fear and anger

Nearly identical results as the whole-brain MAM-ICM pattern similarity analysis were observed when the main analyses were repeated after excluding amygdala voxels (Figure 6).

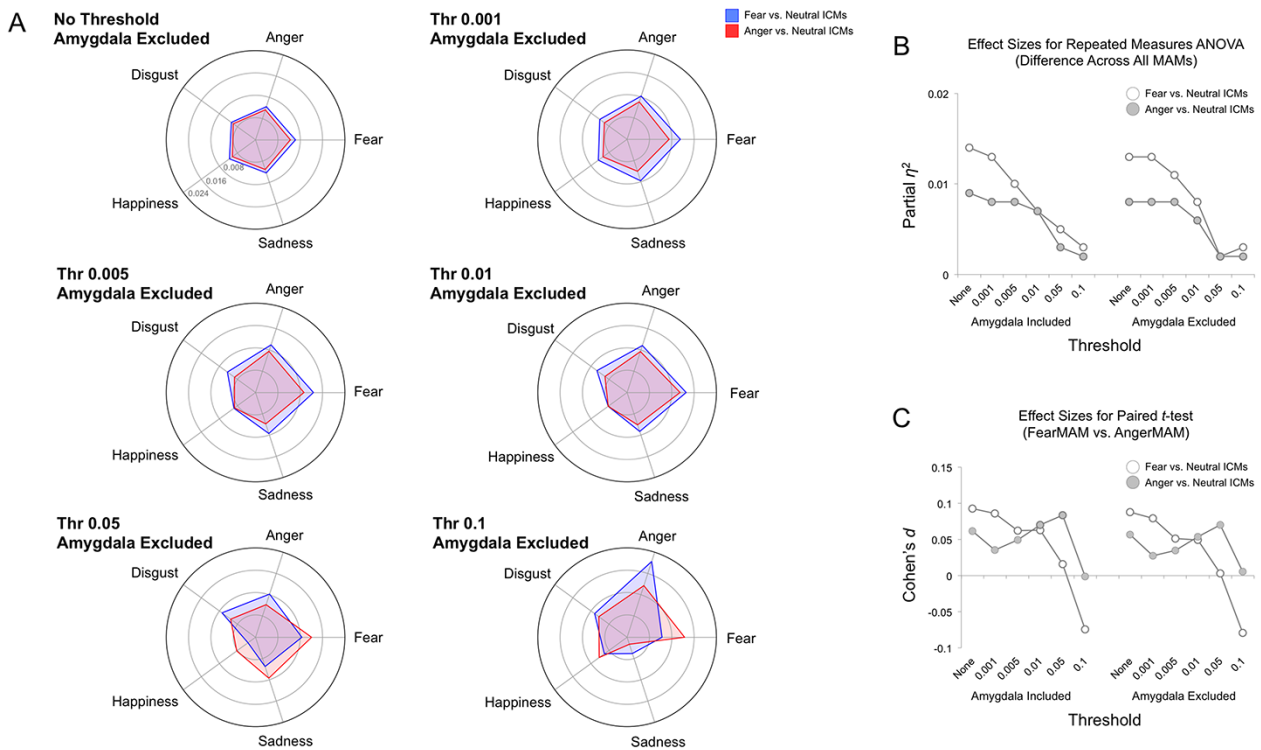


Fig. 6. Non-amygdala MAM-ICM pattern similarity. (A) Pattern similarity measures for ICM-F (blue) and ICM-A (red) and each of the five MAMs, summarized by varying threshold levels. Overall, both ICM-F and ICM-A showed nearly identical results as the whole-brain MAM-ICM pattern similarity analysis that included the amygdala. (B) Plotting the effect sizes from repeated-measures ANOVA showed a gradually declining trend as a function of increased threshold levels. The line graphs on the left depict the results using whole-brain voxels (i.e. amygdala included), and the line graphs on the right show the results using all non-amygdala voxels. (C) A similar trend was found when the effect sizes from paired t-tests were plotted.

Discussion

Here, we compared reference MAMs generated for five distinct categories of emotion with fear and anger ICMs from a large study sample. Contrary to our hypothesis, we found that both ICMs exhibited the greatest pattern similarity to fear MAMs relative to all other MAMs including anger, which may be explained by considering that the ICMs reflect emotion perception, whereas the MAMs represent both emotion perception and expression. The degree of pattern similarity decreased as the number of voxels included in the computation of the MAMs became more selective (i.e. decreased), suggesting that more distributed patterns of brain activity are better reflective of a specific emotion category. Furthermore, amygdala activity associated with either ICM was neither sufficient nor necessary for determining the overall pattern similarity between the ICMs and MAMs.

As predicted, MAM-ICM pattern similarity for fear and anger was significantly greater than zero but generally weak. This may reflect the heterogeneity inherent to the MAMs in comparison with the ICMs. The MAMs were generated from multiple studies that have used heterogeneous stimuli (e.g. faces, pictures, words, films and sounds) that would enable the extraction of a latent neural pattern for a given emotion, whereas the ICMs were strictly based on facial expressions and thus study-specific by nature. Moreover, it is again worth noting that the MAMs include studies that involve different psychological processes with regard to emotion—for example, watching an emotionally charged video clip would likely evoke subjective feelings of such emotion, whereas evaluating still photos of emotional facial expressions rarely would. Thus, the significant yet weak overall

correlation between a given MAM-ICM pair is not surprising, as it may be partly attributable to this qualitative difference across the maps; another plausible reason is the inclusion of likely non-informative, noisy voxels present in the initial analysis with unthresholded MAM-ICM pairs. Yet another possibility is the effect of idiosyncratic brain responses across ICMs, which was supported by a boost in overall pattern similarity with MAMs when aggregated group maps of ICMs (second-level random effects models) were used (see [supplementary data](#)). Regardless, ICM-F did exhibit the greatest pattern similarity with MAM-F as expected. This implies that ICM-F does capture a putative neural correlate of ‘fear’ embedded within distributed brain activity and provides support for the research strategy employed in the present study. In other words, these neural activity patterns indicate responses embedded within brain voxels to the emotion of fear. These could range from a subjective feeling of fear or being in a fearful state (i.e. being afraid) to recognizing fear from another person’s face (i.e. cognitive processing of fear information).

However, ICM-A did not exhibit the greatest pattern similarity with MAM-A. In fact, ICM-A exhibited the greatest pattern similarity to MAM-F. This suggests that the distributed brain activity associated with ICM-A is more similar to neural activity patterns representing fear than anger. While this would appear to be paradoxical, a plausible explanation can be offered by considering the potential differences in the perception *vs* experience of emotions (Lindquist et al., 2012). The key here is the use of angry facial expressions with directed eye-gaze in our emotional face-matching task. Angry faces with eye-gaze oriented toward the perceiver by default signal an impending aggression on the part

of the expressor (Adams et al., 2003; Marsh et al., 2005), which is reflected as differential patterns of brain activity to angry faces with direct gaze vs. averted gaze (Adams et al., 2003; N'Diyae et al., 2009; Ewbank et al., 2010; Ziaei et al., 2016). From the perspective of the perceiver, the primary signal being communicated via angry faces is an increase in the probability of impending threat, not unlike fear faces (Whalen et al., 2001). It follows then that the perceiver's typical response to such angry faces would better align with a threat-related response that is reminiscent of fear more so than anger. Since the MAM-A was generated from individual studies employing not just facial expressions but also other anger-'inducing' stimuli, it can be understood as representing the feeling of anger *per se*, not the response to someone else's anger directed at the perceiver. Thus, the present results showing that ICM-A is more similar to neural activity patterns representing fear than anger could be consistent with brain activity in response to interpersonal threat (i.e. angry faces with gaze directed toward the perceiver). However, an alternative explanation is possible via differences in the decoding performance between MAM-F (86% accuracy) and MAM-A (43% accuracy) documented in the original study (Wager et al., 2015). These authors suggested that this performance difference might be an artifact of relatively greater methodological heterogeneity in research on anger compared to fear (see Supplementary Figure S1 of Wager et al. (2015) for details). Thus, it is possible that this performance discrepancy may be driving the higher pattern similarities between ICM-A and MAM-F in our analyses (i.e. MAM-A might simply be a poorer map). That said, control analyses showed little evidence that surprise ICMs are strongly associated with MAM-F, providing support to the possibility that ICM-F and ICM-A might be converging on a common neural representation of threat embedded within MAM-F (see supplementary data).

These MAM-ICM pattern similarity results were dependent on the number of voxels that were included in the analysis. By systematically manipulating the number of selected voxels, we found that, in general, more voxels yielded better outcomes. Another outcome associated with voxel selection via threshold manipulation is that the range of values that the voxels can assume becomes restricted, which may also have contributed to the smaller effect sizes observed at more stringent threshold levels. However, since the inclusion of all voxels in the brain would necessarily contain those without any informational value (reflected as weak overall MAM-ICM correlations in the unthresholded analysis), additional considerations were warranted. An initial survey of the effect sizes as well as the size of the pattern similarity metrics suggested that a light threshold (0.001–0.005) provides the optimal solution, which still covers a wide range of cortical and subcortical brain regions. The distributed nature of these most informative voxels is consistent with the predictions of the original meta-analysis study (Wager et al., 2015) and generally in line with the constructionist view of emotion (Lindquist et al., 2012; Barrett and Russell, 2015), as well as findings from MVPA research on distinct emotion categories (Peelen et al., 2010; Kassam et al., 2013; Kragel and LaBar, 2015; Saarimäki et al., 2016). Our data offer another piece of evidence that information about emotion categories are distributed, not localized in brain activity.

This interpretation of the present findings is furthered by the amygdala ROI analyses. If we suppose that all of the important information regarding emotion categories was being represented within the amygdala, then restricting the analysis only to the amygdala voxels should have yielded the same MAM-ICM pattern similarity outcomes from the whole-brain analyses. Our data did not support this supposition, further reinforcing the main

result that the inclusion of more voxels across the brain was generally beneficial in matching ICMs with MAMs. Relatedly, it is noteworthy that both MAM-F and MAM-A are characterized by similar patterns of amygdala activity (Wager et al., 2015), which was corroborated by our findings that MAM-F and MAM-A exhibited the greatest similarity over and beyond other MAM pairs (see supplementary data). This suggests the possibility that this shared feature of the MAM-F and MAM-A may drive the pattern similarity with the corresponding ICMs, as both ICM-F and ICM-A are also characterized by increased amygdala activity. Our data rejected this possibility, as excluding the amygdala voxels from the analyses did not change the overall results. In fact, the findings remained remarkably similar to the whole-brain MAM-ICM pattern similarity findings, with minimal changes in *z* scores and effect sizes. This illustrates that the amygdala voxels did not contribute to distinguishing discrete emotion categories in a significant way, and thus, the informational value of the amygdala, at least by itself, was negligible.

Finally, we note that the overall degree of pattern similarity with MAMs increased when using group contrast maps instead of ICMs (see supplementary data). Conceptually, this observation is consistent with the fact that group contrast maps are aggregations of multiple ICMs, which offer a distilled representation of a given brain state similar to MAMs. This intermediate position of the group contrast maps (i.e. averages) between MAMs (i.e. averages of averages) and ICMs (i.e. individuals) could account for the boost in pattern similarity metrics with MAMs. An important issue to consider further is the possibility that group contrast maps—which are designed to remove noise from individual data and provide generalizable brain maps—may also eliminate meaningful individual differences reflected in distributed activity patterns, and if so, to what extent.

The present study is not without limitations. The experimental task from which the ICMs were derived exclusively used facial expressions as the emotional stimuli. While facial expressions are widely used in the literature to examine brain responses to emotion (Costafreda et al., 2008), affective information is represented in the brain in both a modality-specific and modality-general manner (Chikazoe et al., 2014; Shinkareva et al., 2014; Kim et al., 2017); thus, testing the generalizability of the present findings using ICMs derived from other modalities is warranted. It is worth noting yet again that the MAMs used in the present study were generated using individual studies employing heterogeneous stimuli to represent or elicit emotions (e.g. faces, pictures, films and words). Thus, the resulting MAMs may be capturing modality-general neural activity patterns of emotions in the brain. Also, we were only able to focus on the two threat-related emotions (fear and anger), as our emotional face-matching task did not include the three other emotion categories for which there are MAMs. As such, it remains to be seen whether ICMs of other emotions (disgust, happiness and sadness) would show similar mappings onto corresponding MAMs. Next, we observed an unexpected pattern similarity between both ICM-F and ICM-A with MAM-H when the analysis was restricted to amygdala voxels. As there are no known psychological processes that would support this, it is likely that this may simply reflect an artifact stemming from the analyses relying on far fewer voxels with a more restricted range of values. Thus, we are cautious not to overinterpret this observation. We also acknowledge that the effect sizes of the overall pattern similarity between ICMs and the corresponding MAMs are small. A MAM would ideally represent a distilled brain map for a given emotion, whereas an ICM would represent a specific type of affective signal (e.g. fear

information processing from the facial expressions of others) plus the overall brain state that is specific to the task used in our study. The inherent study-specific nature of ICMs may contribute to the small shared variance with MAMs. In our analyses, we tested for linear associations between the voxel values that the MAMs and ICMs assume. While this decision reflects, in part, the proof-of-concept nature of the initial analysis (e.g. fear MAM-ICM pair showing the greatest pattern similarity) as well as previous instances of employing similar approaches and achieving useful findings (e.g. Shahane *et al.*, 2019), we acknowledge the possibility that assuming a linear relationship could be suboptimal, and further investigation on this matter is warranted. Finally, findings from meta-analyses (i.e. MAMs) are inherently bound by the quality of the individual data (Wager *et al.*, 2015). As technical advances in fMRI data acquisition and processing have been made in recent years, it would be worthwhile revisiting the current research topic when updated MAMs that include post-2011 studies become available.

These limitations notwithstanding, our current findings highlight that widely distributed patterns of brain activity from ICMs of threat-related emotion perception, across multiple brain regions and systems, may be best suited for capturing emotion categories identified by MAMs. In contrast, the amygdala was neither sufficient nor necessary for observing such MAM-ICM pattern similarity effects across discrete emotion categories. More generally, the present study offers a strategy that could further boost the utility of MAMs, whose importance has become increasingly recognized in neuroimaging research. For example, MAMs may be used as a guide to chart individual brain states and offer a principled framework for reverse inference from functional neuroimaging data (Poldrack and Yarkoni, 2016). If we have MAMs for fear that tap into different aspects of fear processing, future research can offer a way to harness them and predict what type of psychological state (e.g. feeling afraid vs remembering being afraid) an individual was experiencing during scanning. As such, MAMs may be able to further shed light on the underlying mental processes captured by ICMs, which can contribute to better interpretations of findings using contrast-based task fMRI.

Acknowledgements

We thank the Duke Neurogenetics Study participants as well as the staff of the Laboratory of NeuroGenetics. We also thank the original authors of the meta-analysis maps for their generosity in making them available for use.

Funding

The Duke Neurogenetics Study was supported by Duke University and National Institutes of Health (NIH) grants R01DA031579 and R01DA033369. A.R.H. is further supported by NIH grant R01AG049789. The Duke Brain Imaging and Analysis Center's computing cluster, upon which all DNS analyses heavily rely, was supported by the Office of the Director, NIH, under Award Number S10OD021480.

Conflict of interest

The authors declare that they have no conflict of interest.

Supplementary data

Supplementary data is available at SCAN online.

References

- Adams, R.B., Gordon, H.L., Baird, A.A., Ambady, N., Kleck, R.E. (2003). Effects of gaze on amygdala sensitivity to anger and fear faces. *Science*, **300**, 1536.
- Adolphs, R., Tranel, D., Damasio, H., Damasio, A.R. (1995). Fear and the human amygdala. *Journal of Neuroscience*, **15**, 5879–91.
- Barrett, L.F., Russell, J.A. (2015). *The Psychological Construction of Emotion*. New York: Guilford.
- Barrett, L.F., Satpute, A.B. (2019). Historical pitfalls and new directions in the neuroscience of emotion. *Neuroscience Letters*, **693**, 9–18.
- Chikazoe, J., Lee, D.H., Kriegeskorte, N., Anderson, A.K. (2014). Population coding of affect across stimuli, modalities and individuals. *Nature Neuroscience*, **17**, 1114–22.
- Costafreda, S.G., Brammer, M.J., David, A.S., Fu, C.H.Y. (2008). Predictors of amygdala activation during the processing of emotional stimuli: a meta-analysis of 385 PET and fMRI studies. *Brain Research Reviews*, **58**, 57–70.
- Cox, R.W. (1996). AFNI: software for analysis and visualization of functional magnetic resonance neuroimages. *Computational Biomedical Research*, **29**, 162–73.
- Davis, M., Whalen, P.J. (2001). The amygdala: vigilance and emotion. *Molecular Psychiatry*, **6**, 13–34.
- Eickoff, S.B., Laird, A.R., Grefkes, C., Wang, L.E., Zilles, K., Fox, P.T. (2009). Coordinate-based activation likelihood estimation meta-analysis of neuroimaging data: a random-effects approach based on empirical estimates of spatial uncertainty. *Human Brain Mapping*, **30**, 2907–26.
- Ekman, P. (1992). An argument for basic emotions. *Cognition & Emotion*, **6**, 169–200.
- Ekman, P.F., Friesen, W.V. (1976). *Pictures of Facial Affect*. Palo Alto: Consulting Psychologists Press.
- Ewbank, M.P., Fox, E., Calder, A.J. (2010). The interaction between gaze and facial expression in the amygdala and extended amygdala is modulated by anxiety. *Frontiers in Human Neuroscience*, **4**, 56.
- Fitzgerald, D.A., Angstadt, M., Jelsone, L.M., Nathan, P.J., Phan, K.L. (2006). Beyond threat: amygdala reactivity across multiple expressions of facial affect. *NeuroImage*, **30**, 1441–8.
- Greve, D.N., Fischl, B. (2009). Accurate and robust brain image alignment using boundary-based registration. *NeuroImage*, **48**, 63–72.
- Kassam, K.S., Markey, A.R., Cherkassky, V.L., Loewenstein, G., Just, M.A., Gray, M. (2013). Identifying emotions on the basis of neural activation. *PLoS One*, **8**, e66032.
- Kim, J., Shinkareva, S.V., Wedell, D.H. (2017). Representations of modality-general valence for videos and music derived from fMRI data. *NeuroImage*, **148**, 42–54.
- Kim, M.J., Loucks, R.A., Palmer, A.L., *et al.* (2011). The structural and functional connectivity of the amygdala: from normal emotion to pathological anxiety. *Behavioural Brain Research*, **223**, 403–10.
- Kim, M.J., Scult, M.A., Knodt, A.R., *et al.* (2018). A link between childhood adversity and trait anger reflects relative activity of the amygdala and dorsolateral prefrontal cortex. *Biological Psychiatry: Cognitive Neuroscience and Neuroimaging*, **3**, 644–9.
- Klein, A., Andersson, J., Ardekani, B.A., *et al.* (2009). Evaluation of 14 nonlinear deformation algorithms applied to human brain MRI registration. *NeuroImage*, **46**, 786–802.
- Kober, H., Barrett, L.F., Joseph, J., Bliss-Moreau, E., Lindquist, K., Wager, T.D. (2008). Functional grouping and cortical-subcortical interactions in emotion: a meta-analysis of neuroimaging studies. *NeuroImage*, **42**, 998–1031.

- Kober, H., Wager, T.D. (2010). Meta-analysis of neuroimaging data. *Wiley Interdisciplinary Reviews Cognitive Science*, **1**, 293–300.
- Kragel, P.A., Reddan, M.C., LaBar, K.S., Wager, T.D. (2019). Emotion schemas are embedded in the human visual system. *Science Advances*, **5**, eaaw4358.
- Kragel, P.A., LaBar, K.S. (2015). Multivariate neural biomarkers of emotional states are categorically distinct. *Social Cognitive and Affective Neuroscience*, **10**, 1437–48.
- LeDoux, J.E. (1993). Emotional memory systems in the brain. *Behavioural Brain Research*, **58**, 69–79.
- Lindquist, K.A., Wager, T.D., Kober, H., Bliss-Moreau, E., Barrett, L.F. (2012). The brain basis of emotion: a meta-analytic review. *Behavioral and Brain Sciences*, **35**, 121–43.
- Maren, S. (2001). Neurobiology of Pavlovian fear conditioning. *Annual Reviews of Neuroscience*, **24**, 897–931.
- Marsh, A.A., Ambady, N., Kleck, R.E. (2005). The effects of fear and anger facial expressions on approach- and avoidance-related behaviors. *Emotion*, **5**, 119–24.
- N'Diyae, K., Sander, D., Vuilleumier, P. (2009). Self-relevance processing in the human amygdala: gaze direction, facial expression, and emotion intensity. *Emotion*, **9**, 798–806.
- Nichols, T.E. (2017). Notes on creating a standardized version of DVARS. *arXiv*, 170401469.
- Peelen, M.V., Atkinson, A.P., Vuilleumier, P. (2010). Supramodal representations of perceived emotions in the human brain. *Journal of Neuroscience*, **30**, 10127–34.
- Phelps, E.A., LeDoux, J.E. (2005). Contributions of the amygdala to emotion processing: from animal models to human behavior. *Neuron*, **48**, 175–87.
- Poldrack, R.A., Yarkoni, T. (2016). From brain maps to cognitive ontologies: informatics and the search for mental structure. *Annual Review of Psychology*, **67**, 587–612.
- Power, J.D., Mitra, A., Laumann, T.O., Snyder, A.Z., Schlaggar, B.L., Petersen, S.E. (2014). Methods to detect, characterize, and remove motion artifact in resting state fMRI. *NeuroImage*, **84**, 320–41.
- Russell, J.A. (1980). A circumplex model of affect. *Journal of Personality and Social Psychology*, **39**, 1161–1178.
- Saarimäki, H., Gotsopoulos, A., Jääskeläinen, I.P., et al. (2016). Discrete neural signatures of basic emotions. *Cerebral Cortex*, **26**, 2563–73.
- Shahane, A.D., Lopez, R.B., Denny, B.T. (2019). Implicit reappraisal as an emotional buffer: reappraisal-related neural activity moderates the relationship between inattention and perceived stress during exposure to negative stimuli. *Cognitive, Affective & Behavioral Neuroscience*, **19**, 355–65.
- Shinkareva, S.V., Wang, J., Kim, J., Facciani, M.J., Baucom, L.B., Wedell, D.H. (2014). Representations of modality-specific affective processing for visual and auditory stimuli derived from fMRI data. *Human Brain Mapping*, **35**, 3558–68.
- Tyszka, J.M., Pauli, W.M. (2016). *In vivo* delineation of subdivisions of the human amygdaloid complex in a high-resolution group template. *Human Brain Mapping*, **37**, 3979–98.
- Wager, T.D., Kang, J., Johnson, T.D., Nichols, T.E., Satpute, A.B., Barrett, L.F. (2015). A Bayesian model of category-specific emotional brain responses. *PLoS Computational Biology*, **11**, e1004066.
- Whalen, P.J., Shin, L.M., McInerney, S.C., Fischer, H., Wright, C.I., Rauch, S.L. (2001). A functional MRI study of human amygdala responses to facial expressions of fear vs. anger. *Emotion*, **1**, 70–83.
- Yarkoni, T., Poldrack, R.A., Nichols, T.E., Van Essen, D.C., Wager, T.D. (2011). Large-scale automated synthesis of human functional neuroimaging data. *Nature Methods*, **8**, 665–70.
- Ziaei, M., Ebner, N.C., Burianová, H. (2016). Functional brain networks involved in gaze and emotional processing. *European Journal of Neuroscience*, **45**, 312–20.